Thrombus Imaging with a Technetium-99m-Labeled, Activated Platelet Receptor-Binding Peptide

John Lister-James, Linda C. Knight, Alan H. Maurer, Larry R. Bush, Brian R. Moyer and Richard T. Dean

Diatide, Inc., Londonderry, New Hampshire and Nuclear Medicine Department, Temple University School of Medicine, Philadelphia, Pennsylvania

The objective of this work was the preclinical evaluation of ^{99m}Tc-P280, a ^{99m}Tc-labeled peptide having high affinity and specificity for the GPIIb/IIIa receptor expressed on activated platelets, for use as a thrombus imaging agent. **Methods:** The affinity and specificity of P280 peptide for the GPIIb/IIIa receptor was assessed by the inhibition of ADP-stimulated human platelet aggregation, the inhibition of the binding of fibrinogen to the GPIIb/IIIa receptor and the inhibition of the binding of vitronectin to the vitronectin receptor. P280 peptide was radiolabeled with ^{99m}Tc by ligand exchange using ^{99m}Tc-glucoheptonate. The ability of ^{99m}Tc-P280 to detect thrombi in vivo was assessed using a canine venous thrombosis model and the biodistribution of ^{99m}Tc-P280 was determined in rats and rabbits. **Results:** P280 peptide had an IC_{50} of 79 nM for the inhibition of aggregation of human platelets in platelet rich plasma, an IC_{50} of 6.8 nM for the inhibition of fibrinogen binding to the GPIIb/IIIa receptor and an IC_{50} of 13 μM for the inhibition of vitronectin binding to the vitronectin receptor, showing the high in vitro receptor binding affinity and specificity of the peptide. ^{99m}Tc-P280 was readily prepared in $\geq$90% radiochemical yield and purity and provided images of femoral vein thrombi in the canine model by 1 hr postinjection (thrombus-to-blood ratio of 4.4 and thrombus-to-muscle ratio of 11 at 4 hr). Dog, rat and rabbit studies all showed rapid clearance of the radiotracer from the blood and rapid renal excretion. **Conclusion:** The combination of high in vitro receptor-binding affinity and specificity, in vivo thrombus imaging and fast clearance support the evaluation of ^{99m}Tc-P280 as a clinical imaging agent.

Key Words: thrombosis imaging; activated-platelet imaging; GPIIb/IIIa receptor; technetium-99m-labeled peptide; deep vein thrombosis

J Nucl Med 1996; 37:775–781

Deep vein thrombosis (DVT) and pulmonary embolism (PE) are common clinical conditions that are associated with significant morbidity and mortality. It has been estimated that in the U.S. approximately 5 million patients experience one or more episodes of DVT per year, that over 500,000 cases of pulmonary embolism occur and of these 100,000 deaths result (*1*). It has been estimated that more than 70% of all pulmonary emboli arise from DVT in the lower extremities (*2*). Thus the accurate and timely diagnosis of this condition is an important and recurrent clinical problem.

The diagnostic modality most commonly used to detect DVT is Duplex ultrasonography. This noninvasive procedure has been reported to have excellent sensitivity and specificity in the thigh, but poor accuracy below the knee (*3*) and poor sensitivity in asymptomatic, high-risk patients (*4*). Although the contrast venogram is still considered the most accurate method for detecting DVT, this uncomfortable procedure has significant associated complications and is decreasingly used in the U.S.

Both methods have questionable accuracy in differentiating acute from chronic conditions.

A hot spot scintigraphic thrombus imaging agent has been a long-desired goal (*5*). Radiopharmaceuticals that have been investigated for this use include various radiolabeled plasma proteins and radiolabeled platelets (see reference 6 for a review) but these have suffered from lack of specificity, poor pharmacokinetics or cumbersome radiopharmaceutical preparation (derivation from human blood or involving the manipulation of autologous blood). More recently, both platelet and fibrin-binding radiolabeled murine and human monoclonal antibodies have been examined as thrombus imaging agents, but these also suffer from slow pharmacokinetics and also have a potential for inducing an immune response (see references 6 and 7 for reviews).

Platelets, which are to a greater or lesser extent a component of all thrombi, express the surface membrane glycoprotein IIb/IIIa (GPIIb/IIIa) receptor (*8*). When a platelet becomes activated, for example upon binding to a break in a vessel wall, its GPIIb/IIIa receptors become available for binding fibrinogen (*9*). Fibrinogen binds to the GPIIb/IIIa receptor on activated platelets, but not on unactivated platelets, with moderately high affinity ($Kd \cong 100$ nM)(*10*) and cross-links platelets to form a hemostatic plug (*9*). Thus, an imaging agent which binds specifically to the GPIIb/IIIa receptor on activated platelets would represent a true biochemical marker of the active process in thrombosis.

It has been found that small peptides (less than 20 amino acids) containing the peptide sequence arginine-glycine-aspartate (RGD in single-letter amino acid code) can be constructed such that they bind to the GPIIb/IIIa receptor with a high enough affinity to effectively compete with endogenous fibrinogen (*11*). A suitably radiolabeled peptide that binds with high affinity to the GPIIb/IIIa receptor on activated platelets should provide a means of localizing thrombi anywhere in the body using gamma scintigraphy.

Knight et al. reported being able to detect femoral vein thrombi in a dog model using ^{99m}Tc-labeled GPIIb/IIIa receptor-binding peptides (*12*). However the peptide selected for clinical evaluation (PAC-8) had only modest affinity ($IC_{50} = 12$ μM in an inhibition of platelet aggregation assay, see below) for the GPIIb/IIIa receptor and performed poorly in initial clinical studies (*13*).

We have carried out an extensive structure-activity relationship study of small, synthetic, ^{99m}Tc-labelable, high-affinity GPIIb/IIIa receptor-binding peptides. From that study we have selected the synthetic peptide, P280, which contains an RGD-mimetic sequence, which binds with high affinity to the GPIIb/IIIa receptor, and which when labeled with ^{99m}Tc, provides ^{99m}Tc-P280, a new radiopharmaceutical for the non-invasive detection of thromboembolism. This report describes the preclinical evaluation of ^{99m}Tc-P280.

MATERIALS AND METHODS

P280 Peptide Trifluoroacetate

P280 peptide trifluoroacetate salt was prepared by solid-phase peptide synthesis using an ABI 431A peptide synthesizer, ABI FastMoc™ chemistry and Rink amide resin (Advanced Chem Tech, Louisville, KY). The peptide was purified by preparative C_{18} reversed-phase HPLC using a Delta-Pak C_{18}, 15 μm, 300 Å, 47 × 300 mm column (Waters Chromatography, Millipore Corp., Milford, MA) and 0.1% trifluoroacetic acid in water (0.1% TFA/H_2O) modified with 0.1% trifluoroacetic acid in 90% acetonitrile/10% water (0.1% TFA/(90% CH_3CN/H_2O)) as eluents, and then lyophilized. The identity of the P280 peptide trifluoroacetate was confirmed by amino acid analysis and electrospray mass spectrometry (ESMS). P280 peptide purity was determined by analytical C_{18} reversed-phase HPLC in two different solvent systems and peptide content was determined by analysis of total nitrogen.

Technetium-99m-Radiolabeling

Peptide P280 was labeled with ^{99m}Tc by ligand exchange using ^{99m}Tc-glucoheptonate as ligand exchange reagent. Thus, P280 peptide trifluoroacetate was dissolved to 1 mg/ml in 0.9% saline. Technetium-99m glucoheptonate was prepared by reconstituting a Glucoscan® vial (DuPont Pharma, Billerica, MA) with 1.0 ml of ^{99m}Tc sodium pertechnetate containing up to 7.4 GBq (200 mCi) and allowed to stand for 15 min at room temperature. To each ml of peptide solution was added 250 μl of ^{99m}Tc-glucoheptonate, the reaction was allowed to proceed at 100°C for 15 min and then the solution was allowed to cool to room temperature and filtered through a 0.22-μm low protein-binding filter.

Radiochemical yield and purity were determined by instant thin-layer chromatography (ITLC) using saturated saline (^{99m}Tc-P280, and ^{99m}Tc-microcolloid remain immobile, other species are mobile) and water (^{99m}Tc-microcolloid immobile, all other species, including ^{99m}Tc-P280, are mobile) as developing solvents.

Radiometric-HPLC was performed using an HPLC equipped with an in-line gamma detector linked to an integrating recorder, an analytical reversed-phase column (Delta-Pak C18, 5 μM, 300 Å, 3.9 × 150 mm) eluted at 1.2 ml/min with a gradient of 0.1% TFA/H_2O to 0.1% TFA/(90% CH_3CN/H_2O) over 20 min.

In Vitro Assays

Inhibition of Human Platelet Aggregation. Peptide P280 was evaluated in vitro for inhibition of platelet aggregation essentially as described by Zucker (*14*). Each assay used fresh human platelet-rich plasma at approximately 300,000 platelets per μl. Aggregation of platelets was induced by 10 or 15 μM ADP and was measured using a Bio/Data aggregometer. The concentration of P280 peptide was varied from 500 to 0.1 μg per ml. The concentration of peptide which reduced platelet aggregation by

50% (IC_{50}) was determined from plots of percent aggregation versus peptide concentration (inhibition curves).

Inhibition of Binding of Fibrinogen to GPIIb/IIIa Receptors and of Vitronectin Binding to Vitronectin Receptors (Vnr). These assays were performed as has been reported (*15,16*). Briefly, the assays were set up as competitions between P280 peptide and either soluble GPIIb/IIIa or Vnr preparations for either fibrinogen or vitronectin bound to plastic multiwell plates. Bound GPIIb/IIIa or Vnr were assayed using mouse antireceptor antibodies and then HRP conjugates of either rabbit or goat antimouse antibodies.

Animal Model

Technetium-99m-P280 was evaluated in vivo in an animal model which has been reported previously for the evaluation of thrombus imaging radiotracers (*12,17,18*). Mongrel dogs (13 to 26 kg, fasted overnight) were sedated (ketamine and acepromazine intramuscularly) then anesthetized intravenously with sodium pentobarbital. In each animal, an 18-gauge angiocath was inserted into the distal half of the right femoral vein and an 8-mm dacron-entwined stainless steel embolization coil (Cook Co., Bloomington, IN) was placed in the femoral vein at approximately the mid-femur. The catheter was removed, the wound was sutured and the placement of the coil was documented by radiography. The animals were allowed to recover overnight.

Imaging Studies

On the day following coil placement, each animal was reanesthetized, intravenous saline drips were placed in each foreleg and a urinary bladder catheter was inserted to collect urine. The animal was placed supine under a gamma camera (GE MaxiCamera, Milwaukee, WI) which was equipped with a low-energy, all-purpose collimator and set to acquire the 140 keV photopeak of ^{99m}Tc with a 20% window. Images were acquired on a NucLear Mac computer system (Scientific Imaging, Denver, CO).

In 6 dogs, ^{99m}Tc-P280 (185–370 MBq (5–10 mCi) ^{99m}Tc and 0.2–0.4 mg peptide) was injected intravenously as a bolus into a foreleg line and flushed in with saline.

As a positive control, three dogs were studied with ^{99m}Tc-HMPAO-labeled autologous platelets (*19*) (260 MBq; 7 mCi) and as a negative control, two dogs were studied with ^{99m}Tc-glucoheptonate (290 MBq; 8 mCi).

Gamma camera imaging was started simultaneously with injection. Anterior images over the heart (64 × 64 byte matrix) were acquired as a dynamic study (10-sec image acquisitions) over the first 10 min then as static images at 1, 2, 3 and 4 hr postinjection. Anterior 128 × 128 byte images over the legs were acquired for 500,000 counts or 20 min, whichever came sooner, at 12 min and at approximately 1, 2, 3 and 4 hr postinjection. Leg images were collected with a lead shield placed over the bladder.
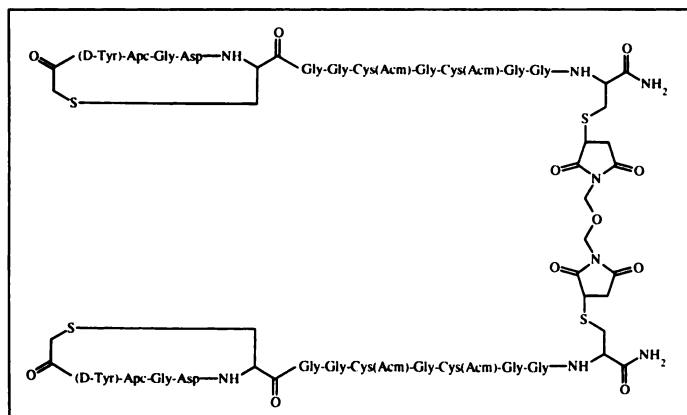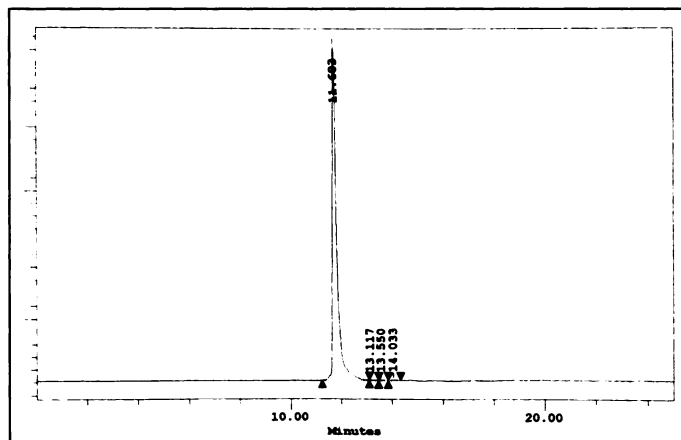

FIGURE 1. P280.

FIGURE 2. ^{99m}Tc-P280 HPLC radiometric trace.

TABLE 1

Percent Injected Dose per Gram in Selected Tissue and ROI Data at 4 Hours in the Canine Venous Thrombosis Model (mean ± s.e.)

Compound	%ID/g Thrombus	%ID/g Blood	Thrombus-to-Blood	Thrombus-to-Muscle	Thrombus/Vessel (ROI)	Thrombus/Muscle (ROI)
[99m]Tc-P280	0.0059 ± 0.0025	0.0012 ± 0.0003	4.4 ± 0.74	11.0 ± 7.0	2.0 ± 0.1	1.9 ± 0.1
[99m]Tc-glucoheptonate	0.0026 ± 0.0002	0.0015 ± 0.0007	2.2 ± 0.8	4.3 ± 2.4	1.5 ± 0.0	1.6 ± 0.1
[99m]Tc-platelets	0.18 ± 0.08	0.037 ± 0.006	5.4 ± 3.2	230.0 ± 100.0	1.8 ± 0.6	5.0 ± 2.2

From the computer-stored images, thrombus-to-background ratios were determined. Average counts per pixel were computed from regions-of-interest (ROIs) drawn manually around the areas of known thrombus (corresponding to the locations of the coils in the radiographs). Similarly, ROIs were drawn over the contralateral femoral vein to estimate blood background and ROIs were drawn over both medial and lateral thigh in the thrombus-containing leg to estimate muscle background. Thrombus-to-background ratios were determined by dividing mean counts per pixel for thrombus by mean counts per pixel for blood or for muscle (average of medial and lateral ROIs).

Thrombus and Tissue Uptake Determinations

Following the final image each animal was deeply anesthetized with pentobarbital. Two blood samples were collected by cardiac puncture using a heparinized syringe followed by a euthanasing dose of saturated potassium chloride solution administered by intracardiac or bolus intravenous injection. The femoral vein containing the thrombus, a similar section of vein of the contralateral (control) leg, and samples of thigh muscle were carefully dissected out. The thrombus, coil and coil fibers were dissected free of the vessel. The thrombus, saline-washed vessel samples, coil and coil dacron fibers were separated, weighed and, along with known fractions of the injected doses, were counted in a gamma well counter in the ^{99m}Tc channel.

Fresh thrombus weight, percent injected dose (%ID)/g in the thrombus and blood obtained just prior to euthanasia, %ID in the coil, excised blood vessels, urine and blood were determined. Thrombus-to-blood and thrombus-to-muscle ratios were calculated from %ID/g values.

Biodistribution Studies in Rats and Rabbits

Normal Sprague-Dawley rats were restrained and injected intravenously via the lateral tail vein with ^{99m}Tc-P280 (40–110 MBq (1–3 mCi) per kg ^{99m}Tc, 0.04–0.06 mg P280 peptide per kg). Groups of three animals were killed by cervical dislocation at 5, 30, 60 and 120 min and necropsied. Samples of blood and excised tissues (rinsed with saline and blotted dry) were weighed and, along with a known fraction of the injected dose, were counted in a well-counter photopeaked for [99m]Tc. The carcasses were counted in the dose calibrator using the ^{99m}Tc setting.

A group of 15 New Zealand White rabbits (2.6–3.4 kg) were sedated and injected intravenously via a marginal ear vein with
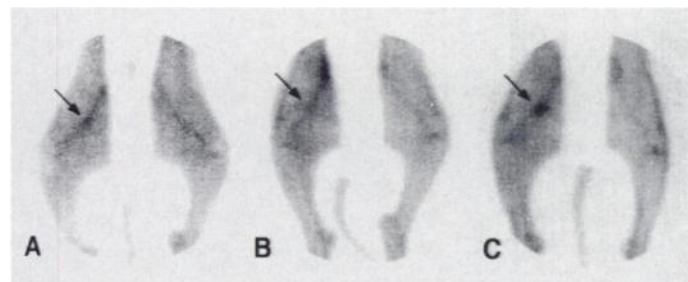
[99m]Tc-P280 (40–70 MBq (1–2 mCi) per kg ^{99m}Tc, 5 μg P280 peptide per kg). Groups of three animals were sacrificed by overdose of Nembutal at 5, 30, 60, 120 and 240 min and necropsied. Samples of blood, bile and excised tissues (rinsed with saline and blotted dry) were weighed and, along with a known fraction of the injected dose, were counted in a well-counter photopeaked for [99m]Tc.

All animal studies were conducted in accordance with NIH guidelines and under IACUC-approved protocols.

RESULTS

P280 Peptide Trifluoroacetate

The structure of P280 is shown in Figure 1. The purity of the P280 peptide trifluoroacetate was ≥90% by HPLC. Amino acid analysis showed the expected ratios of Gly (12), Asp (2) and Tyr (2); Apc and Cys were not assayed. Electrospray mass spectroscopy gave M = 3020, in agreement, within the experimental error of ± 1 amu, with the calculated molecular weight (for $C_{112}H_{162}N_{36}O_{43}S_{10}$) of 3021.

Technetium-99m-P280

P280 was readily labeled by ligand exchange using ^{99m}Tc-glucoheptonate. Radiochemical yield was routinely ≥90% with a specific activity of approximately 60 Ci/mmol P280 Peptide. Radiochemical purity was ≥90% by ITLC and HPLC analysis. An example of an HPLC trace of ^{99m}Tc-P280 is shown in Figure 2. In this system, ^{99m}Tc-P280 had a retention time of 11.7 min. Technetium-99m-pertechnetate and ^{99m}Tc-glucoheptonate eluted within 2 min.

In Vitro Assays

Inhibition of Platelet Aggregation Assay. Inhibition curves from assays of 6 lots of P280 peptide were constructed. The concentration of P280 peptide required to inhibit 50% of human platelet aggregation (IC_{50}) in PRP was 0.079 ± 0.017 μM (mean ± s.d. of 6 lots of peptide).

In a comparison of the potency of P280 peptide in inhibiting the aggregation of dog versus human platelets, IC_{50}s of 0.20 ± 0.11 μM (mean ± s.d.; 6 measurements) and 0.056 ± 0.011 μM (mean ± s.d.; 3 measurements) were measured for dog and human platelets, respectively. Thus, P280 peptide was 2.5 to 3.5

FIGURE 3. ^{99m}Tc-P280 canine DVT model imaging study. (A) 13-min image of hind legs; (B) 1-hr image of hind legs; and (C) 2-hr image of hind legs. Arrows indicate the location of the thrombogenic coil.

FIGURE 4. ^{99m}Tc-glucoheptonate in the canine DVT model (2-hr image). The arrow indicates the location of the thrombogenic coil.
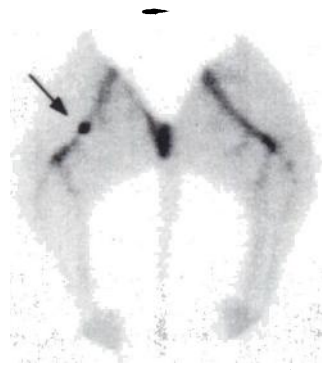
FIGURE 5. ^{99m}Tc-HMPAO-labeled platelets in the canine DVT model (2-hr image). The arrow indicates the location of the thrombogenic coil.

times more potent in inhibiting human platelet aggregation than in inhibiting dog platelet aggregation.

Inhibition of Binding of Fibrinogen to GPIIb/IIIa and Vitronectin to Vnr. P280 inhibited the binding of fibrinogen to a GPIIb/IIIa receptor preparation with an IC_{50} = 6.8 nM. In contrast, P280 had an IC_{50} = 12,900 nM for binding to the vitronectin receptor, thus showing a 3-log selectivity for the GPIIb/IIIa receptor over the vitronectin receptor.

In Vivo Results

Thrombus size in this model averaged 89 ± 26 mg (mean ± s.e.m.). At approximately 4 hr postinjection, percent of injected dose (%ID) in the thrombi averaged 0.00022%, with an approximately equal amount (0.00027%) in the (micro-thrombi attached to the) dacron fibers, but with little (0.000032%) adhering to the coil. Percent ID in the blood (based on 7% of body weight) at sacrifice was 1.4%. As shown in Table 1, ^{99m}Tc-P280 gave 0.0059%ID/g in the thrombi, slightly less (0.0040 %ID/g) in the vessels which contained the thrombi and thrombus-to-blood and thrombus-to-muscle ratios of 4.4 and 11. In comparison, ^{99m}Tc-glucoheptonate, studied as a negative control in 2 dogs, gave much lower uptake (0.0026%ID/g) in the thrombus and lower thrombus-to-blood and thrombus-to-muscle ratios (2.2 and 4.3, respectively). Technetium-99m-HMPAO-labeled autologous platelets gave a much higher %ID/g in thrombi and thrombus-to-muscle, but only a slightly higher thrombus-to-blood ratio than ^{99m}Tc-P280.

An example of images acquired with ^{99m}Tc-P280 are shown in Figure 3. The images were asymmetric (more activity in the thrombosed vessel) as early as 13 min postinjection, with improving thrombus definition over the course of the study. For comparison, images of ^{99m}Tc-glucoheptonate and ^{99m}Tc-HMPAO-platelets are provided as Figures 4 and 5, respectively. As expected, ^{99m}Tc-glucoheptonate did not image the thrombus. Technetium-99m-HMPAO platelets gave excellent images of venous thrombi in this model but, as discussed previously, radiolabeled platelets have slow pharmacokinetics which detract from their utility as clinical imaging agents.

Blood clearance was determined in three dogs by an ROI over the heart from frames collected during the dynamic studies. The results are shown in Figure 6. The blood clearance of ^{99m}Tc-P280 was rapid with apparent first-order kinetics. ROI analysis also showed that ^{99m}Tc-P280 cleared rapidly from the kidneys and the liver as shown (for one animal) in Figure 7.

The results of the biodistribution studies of ^{99m}Tc-P280 in rats and rabbits confirmed the biodistribution observed qualitatively in the dog. The results in rats are shown in Table 2. Circulating activity decreased rapidly over 2 hr (the fraction of the dose in the blood, assumed to be 6% of body weight, at 2 hr was 4% of that at 5 min). The decrease in the recovery of
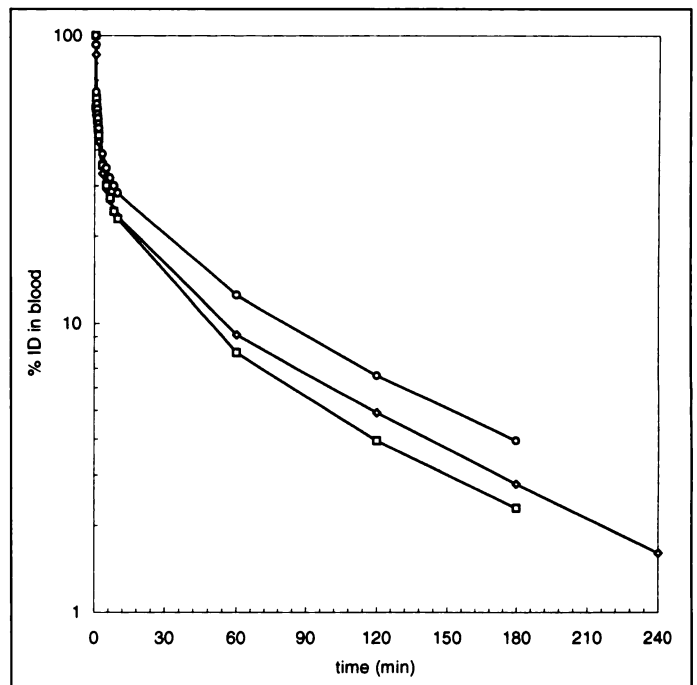

FIGURE 6. Heart blood-pool clearance of ^{99m}Tc-280 in three canine model studies by ROI analysis.

radioactivity in the carcass and tissues with time provided a measure of the rapid excretion of the radiotracer (70% cleared by 2 hr). As there was no substantial gastrointestinal tract uptake observed at any time, excretion was assumed to be primarily renal without substantial renal retention.

The results in rabbits are shown in Table 3. Circulating activity again decreased rapidly over the 4-hr study. Although activity was present in the bile in the gall bladder, and a small amount of uptake was observed in the colon, the transit of activity through the gastrointestinal tract, normally characteristic of hepatobiliary clearance, was not seen. Again the data showed rapid renal clearance (approximately 70% ID in the urine by 4 hr) with only a small amount of retention in the kidneys.

DISCUSSION

Current methods of diagnosing DVT are either invasive (venography), not accurate in all areas of potential thrombosis (ultrasonography) or do not provide information in a timely manner (radiolabeled platelets and antibodies).
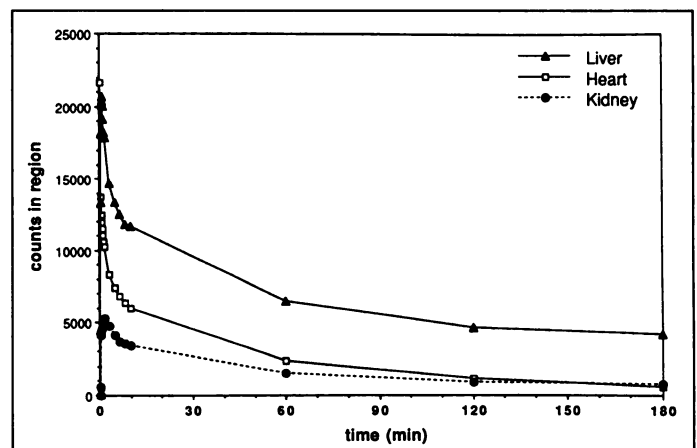

FIGURE 7. Heart blood-pool, liver and kidney clearance of ^{99m}Tc-280 in a canine model study by ROI analysis.

TABLE 2
Biodistribution of Technetium-99m-P280 in the Rat (mean ± s.d.)

Organ	5 Min %ID/g	5 Min %ID	30 Min %ID/g	30 Min %ID	60 Min %ID/g	60 Min %ID	120 Min %ID/g	120 Min %ID
Blood	3.0 ± 0.43	37 ± 4.5	0.70 ± 0.17	8.5 ± 2.0	0.34 ± 0.22	4.4 ± 2.9	0.14 ± 0.038	1.6 ± 0.36
Liver	0.25 ± 0.032	2.1 ± 0.060	0.083 ± 0.020	0.71 ± 0.20	0.041 ± 0.018	0.37 ± 0.17	0.064 ± 0.050	0.50 ± 0.43
Kidney	9.4 ± 3.3	19 ± 6.7	2.7 ± 0.95	5.5 ± 2.1	1.0 ± 0.57	2.0 ± 1.1	3.2 ± 4.2	7.1 ± 9.5
Spleen	0.92 ± 0.22	0.56 ± 0.12	0.40 ± 0.11	0.29 ± 0.13	0.11 ± 0.060	0.066 ± 0.038	0.083 ± 0.032	0.039 ± 0.013
Small intestine		2.0 ± 0.48		1.5 ± 0.24		1.8 ± 1.5		3.8 ± 1.0
Large intestine	—	1.6 ± 0.31	—	0.78 ± 0.47	—	0.22 ± 0.12	—	0.50 ± 0.43
Muscle	0.65 ± 0.060	—	0.39 ± 0.28	—	0.11 ± 0.020	—	0.073 ± .039	—
Carcass	—	56 ± 4.0	—	30 ± 0.77	—	23 ± 14	—	9.1 ± 4.2
Recovery	—	120 ± 13	—	66 ± 6.8	—	35 ± 21	—	29 ± 21

Venous thrombi are fibrin-rich (20), but actively thrombosing venous thrombi also incorporate platelets. Upon binding to fibrin or the blood vessel wall, platelets become activated. In this condition the cell surface membrane GPIIb/IIIa receptors either change conformation or their micro-environment changes (21) and they become available for binding fibrinogen. Fibrinogen binds to the GPIIb/IIIa receptor on activated platelets, but not on unactivated platelets, and cross-links platelets to form or propagate a thrombus (9).

A number of compounds, predominantly peptides, have been discovered which bind to the GPIIb/IIIa receptor via the peptide sequence -Arg-Gly-Asp-(RGD) or a mimetic thereof and inhibit the binding of fibrinogen (15,22–30). Fibrinogen is normally present in plasma at a concentration of 4–10 μM and binds to isolated GPIIb/IIIa receptors with a K_D of approximately 100 nM (10). Small, RGD-containing peptides bind weakly to the GPIIb/IIIa receptor. Thus, Arg-Gly-Asp-Val (RGDV) inhibits the binding of ^{125}I-fibrinogen to platelets with a Ki = 15 μM

TABLE 3
Biodistribution of Technetium-99m-P280 in the Rabbit (mean ± s.d.)

Organ	5 Min %ID/g	5 Min %ID	30 Min %ID/g	30 Min %ID	1 Hr %ID/g	1 Hr %ID
Blood	0.16 ± 0.046	29 ± 7.1	0.071 ± 0.008	13 ± 1.5	0.050 ± 0.014	9.4 ± 1.8
Liver	0.070 ± 0.013	6.1 ± 2.1	0.043 ± 0.007	4.2 ± 1.0	0.030 ± 0.011	2.9 ± 0.24
Kidneys	0.40 ± 0.14	5.1 ± 1.2	0.18 ± 0.035	2.7 ± 0.50	0.13 ± 0.048	2.1 ± 0.55
Spleen	0.040 ± 0.007	—	0.025 ± 0.003	—	0.020 ± 0.005	—
Lungs	0.10 ± 0.018	0.41 ± 0.046	0.045 ± 0.009	0.51 ± 0.030	0.030 ± 0.015	0.17 ± 0.034
Heart	0.070 ± 0.015	0.10 ± 0.004	0.029 ± 0.005	0.11 ± 0.038	0.020 ± 0.007	0.070 ± 0.003
Gall bladder contents	0.11 ± 0.047	—	0.083 ± 0.040	—	0.050 ± 0.026	—
Muscle*	—	23 ± 5.7	—	15 ± 3.5	—	8.1 ± 2.2
Stomach[†]	—	1.4 ± 0.37	—	2.2 ± 1.3	—	2.4 ± 0.48
Duodenum[†]	—	0.39 ± 0.017	—	0.65 ± 0.17	—	0.19 ± 0.074
Jejunum[†]	—	0.88 ± 0.039	—	1.0 ± 0.40	—	0.31 ± 0.15
Ileum[†]	—	0.64 ± 0.028	—	0.49 ± 0.11	—	1.5 ± 0.85
Colon[†]	—	4.1 ± 0.18	—	4.2 ± 0.59	—	6.5 ± 0.33
Urinary bladder[†]	—	0.54 ± 0.024	—	11 ± 1.5	—	23 ± 2.2
Recovery	—	72 ± 16	—	51 ± 1.2	—	56 ± 1.8

Organ	2 Hr %ID/g	2 Hr %ID	4 Hr %ID/g	4 Hr %ID
Blood	0.040 ± 0.010	6.2 ± 1.5	0.030 ± 0.010	5.7 ± 2.2
Liver	0.030 ± 0.009	2.4 ± 0.64	0.030 ± 0.008	2.4 ± 0.82
Kidneys	0.070 ± 0.050	1.1 ± 0.10	0.090 ± 0.030	1.5 ± 0.59
Spleen	0.010 ± 0.003	—	0.10 ± 0.003	—
Lungs	0.030 ± 0.004	—	0.020 ± 0.006	0.14 ± 0.057
Heart	0.020 ± 0.003	—	0.010 ± 0.004	0.010 ± 0.005
Gall bladder contents	0.17 ± 0.098	—	0.14 ± 0.057	—
Muscle*	—	5.7 ± 2.4	—	6.3 ± 3.4
Stomach[†]	—	3.5 ± 1.8	—	1.2 ± 0.40
Duodenum[†]	—	0.17 ± 0.045	—	0.45± 0.26
Jejunum[†]	—	0.24 ± 0.043	—	0.88 ± 0.46
Ileum[†]	—	0.47 ± 0.23	—	2.6 ± 2.9
Colon[†]	—	6.4 ± 2.3	—	6.7 ± 1.9
Urinary bladder[†]	—	42 ± 1.7	—	37 ± 2.4
Recovery	—	68 ± 16	—	65 ± 24

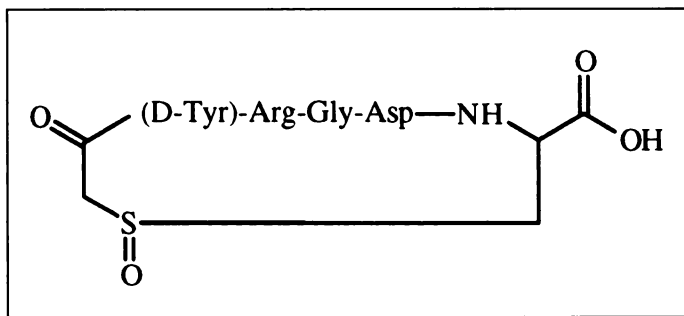*Assumed to be 44% of body weight.
[†]including contents.

FIGURE 8. G-4120.

and inhibits the ADP-induced aggregation of platelets in platelet-rich plasma (which results from the binding of fibrinogen to the GPIIb/IIIa receptors on the activated platelets and consequent platelet aggregation) with an IC_{50} of 130 μM (22,24). A series of large oligopeptides (50 to 70 amino acid residue) derived from snake venoms, known as the disintegrins, bind to the GPIIb/IIIa receptor with much higher affinity. Thus kistrin and echistatin inhibit platelet aggregation in PRP with IC_{50}s of 150 and 80 nM, respectively, approximately 3 logs more potent than RGDV (27,31). The reason for the difference in potency is believed to be a result of the conformational constraint of the RGD sequence in the disintegrins (32). A number of small, synthetic peptides and peptidomimetic compounds have been prepared in which the RGD sequence or a RGD-mimetic sequence is conformationally constrained and which also bind with high affinity to the GPIIb/IIIa receptor and are extremely potent in inhibiting the aggregation of platelets in PRP (16,23,28,30).

Peptide P280 was designed to incorporate the RGD-mimetic sequence -Apc-Gly-Asp in a conformationally constrained cyclic sulfide. The synthetic amino acid Apc, S-aminopropyl-L-cysteine, is an arginine surrogate which not only replaces arginine in the receptor-binding sequence, but confers additional selectivity on the molecule. Thus, P280 peptide has an IC_{50} of 6.8 nM for inhibition of binding of fibrinogen to GPIIb/IIIa and an IC_{50} of 12,900 nM for inhibition of binding of vitronectin to the vitronectin receptor, showing a 3-log selectivity for the GPIIb/IIIa receptor over the vitronectin receptor. In contrast, peptide G-4120 (Figure 8), which contains a cyclic structure similar to that in P280 but contains arginine in place of Apc, has approximately equivalent IC_{50}s of 8.3 nM and 21 nM in the two assays (15). Thus, ^{99m}Tc-P280 would be expected to have a higher selectivity in vivo for the GPIIb/IIIa receptor of activated platelets over other integrin receptors than would RGD-containing peptides. This receptor-selectivity is important for specificity of binding to and imaging activated platelets. For example the vitronectin receptor is present on platelets, endothelial cells, smooth muscle cells and macrophages (32), does not require platelet activation to bind ligands and therefore would represent a potential site of non-thrombus localization for a ligand that was not GPIIb/IIIa receptor-specific.

Furthermore P280 peptide inhibits the aggregation of human platelets in platelet rich plasma with an IC_{50} of 79 nM. This is of the order of potency of the snake venom peptide echistatin [IC_{50} = 80 nM (25)] which is one of the most potent known naturally-occurring fibrinogen antagonists. Thus P280 peptide has both high affinity and high selectivity for the GPIIb/IIIa receptor. This is in contrast to peptides previously investigated for thrombus imaging which were considerably less potent [PAC-8 had an IC_{50} of 12,000 nM for inhibition of human platelet aggregation in PRP (12)].

The results of studies of ^{99m}Tc-P280 in a canine model of DVT confirmed the expectations from the in vitro results, providing in vivo visualization of thrombi and good thrombus-to-blood and thrombus-to-muscle ratios. It is noted that since P280 peptide showed greater potency in inhibiting the aggregation of human versus dog platelets, the performance of ^{99m}Tc-P280 in localizing to and imaging thrombi in humans would be expected to be even better than observed in the dog model. In addition, the fast plasma clearance and predominantly renal excretion of ^{99m}Tc-P280 are pharmacokinetic characteristics favorable for the rapid delineation of thrombi in vivo without interfering background activity and for low absorbed radiation dose.

In fact the predictions from these preclinical studies have been upheld in initial clinical studies in which ^{99m}Tc-P280 has provided excellent images of DVT within 2 hr of injection (33,34).

CONCLUSION

The combination of high in vitro receptor-binding affinity, in vivo thrombus definition and fast clearance indicate that ^{99m}Tc-P280 warrants further clinical evaluation as a thrombus imaging agent.

REFERENCES

1. Anderson FA, Wheeler HB, Goldberg RT, et al. A population-based perspective of the hospital incidence and case facility rates of deep vein thrombosis and pulmonary embolism. *Ann Intern Med* 1991;151:933–938.
2. Hull RD, Hirsh J, Carter CJ, et al. Pulmonary angiography, ventilation lung scanning and venography for clinically suspected pulmonary embolism with abnormal perfusion lung scan. *Ann Intern Med* 1983;98:891–899.
3. Rose SC, Zwiebel WJ, Nelson BD, et al. Symptomatic lower extremity deep venous thrombosis: accuracy, limitations and role of color duplex flow imaging in diagnosis. *Radiology* 1990;175:639–644.
4. Davidson BL, Elliott CG, Lensing AWA. Low accuracy of color Doppler ultrasound in the detection of proximal leg vein thrombosis in asymptomatic high-risk patients. *Ann Intern Med* 1992;117:735–738.
5. Som P, Oster ZH. Thrombus-specific imaging: approaching the elusive goal. *J Nucl Med* 1994;35:202–203.
6. Knight LC. Radiopharmaceuticals for thrombus detection. *Semin Nucl Med* 1990;20:52–67.
7. Koblik PD, De Nardo GL, Berger HJ. Current status of immunoscintigraphy in the detection of thrombosis and thromboembolism. *Semin Nucl Med* 1989;19:221–237.
8. Kieffer N, Phillips DR. Platelet membrane glycoproteins: functions in cellular interactions. *Ann Rev Cell Biol* 1990;6:329–357.
9. Hawiger J. Adhesive interactions of blood cells and the vessel wall. In: Coleman R, Hirsh J, Marder V, Salzman E, eds. *Hemostasis and thrombosis. Basic principles and clinical practice*, 2nd ed. Philadelphia: JB Lippincott Co.; 1987:182–209.
10. JS Bennett, G Vilaire. Exposure of platelet fibrinogen receptors by ADP and epinephrine. *J Clin Invest* 1979;64:1393–1401.
11. Ruggeri ZM, Houghten RA, Russell SR, Zimmerman TS. Inhibition of platelet function with synthetic peptides designed to be high-affinity antagonists of fibrinogen binding to platelets. *Proc Natl Acad Sci USA* 1986;83:5708–5712.
12. Knight LC, Radcliffe R, Maurer AH, Rodwell JD, Alvarez VL. Thrombus imaging with technetium-99m synthetic peptides based upon the binding domain of a monoclonal antibody to activated platelets. *J Nucl Med* 1994;35:282–288.
13. Ben-Haim S, Kahn D, Weiner GJ, et al. The safety and pharmacokinetics in adult subjects of an intravenously administered ^{99m}Tc-labeled 17 amino acid peptide (CYT-379). *Nucl Med Biol* 1994;21:131–142.
14. Zucker MB. Platelet aggregation measured by the photometric method. *Meth Enzymol* 1989;169:117–133.
15. Barker PL, Bullens S, Bunting S, et al. Cyclic RGD peptide analogues as antiplatelet antithrombotics. *J Med Chem* 1992;35:2040–2048.
16. Burnier JP, Gadek T, McDowell R. Platelet aggregation inhibitors having high specificity for GPIIb/IIIa. *Int Pat Appl Pub No.* WO 92/17492; Geneva, Switzerland; 1992.
17. Knight LC, Maurer AH, Ammar IA, Epps LA, Dean RT, Pak KY, Berger HJ.

^{99m}Tc-antifibrin Fab' fragments for imaging venous thrombi: evaluation in a canine model. *Radiology* 1989;173:163–169.

18. Knight LC, Abrams MJ, Schwartz DA, Hauser MM, Kollman M, Gaul FE, Rauh DA. Preparation and preliminary evaluation of technetium-99m-labeled Fragment E_1 for thrombus imaging. *J Nucl Med* 1992;33:710–715.

19. Becker W, Borner W, Borst U. Technetium-99m-hexamethylpropyleneamineoxime (HMPAO) as a platelet label: evaluation of labeling parameters and first in vivo results. *Nucl Med Commun* 1988;9:831–842.

20. Freiman DG. The structure of thrombi. In: Coleman R, Hirsh J, Marder V, Salzman E, eds. *Hemostasis and thrombosis. Basic principles and clinical practice*, 2nd ed. Philadelphia: JB Lippincott Co.; 1987:1123–1135.

21. Coller BS. Activation affects access to the platelet receptor for adhesive glycoproteins. *J Cell Biol* 1986;103:451–456.

22. Plow EF, Pierschbacher MD, Ruoslahti E, Marguerie GA, Ginsberg MH. The effect of Arg-Gly-Asp-containing peptides on fibrinogen and von Willebrand factor binding to platelets. *Proc Natl Acad Sci USA* 1985;82:8057–8061.

23. Samanen J, Ali F, Romoff T, et al. Development of a small RGD peptide fibrinogen receptor antagonist with potent antiaggregatory activity in vitro. *J Med Chem* 1991;34:3114–3125.

24. Alig L, Edenhofter A, Hadvary P, et al. Low molecular weight, nonpeptide fibrinogen receptor antagonists. *J Med Chem* 1992;35:4393–4407.

25. Zablocki JA, Miyano M, Garland RB, et al. Potent in vitro and in vivo inhibitors of platelet aggregation based upon the Arg-Gly-Asp-Phe sequence of fibrinogen. A proposal on the nature of the binding interaction between the Arg-guanidine of RGDX mimetics and the platelet GP IIb/IIIa receptor. *J Med Chem* 1993;36:1811–1819.

26. Cook NS, Bruttger O, Pally C, Hagenbach A. The effects of two synthetic glycoprotein IIb/IIIa antagonists, Ro 43-8857 and L-700,462, on platelet aggregation and bleeding in guinea pigs and dogs: evidence that Ro 43-8857 is orally active. *Throm Haemostasis* 1993;70:838–847.

27. Ramjit DR, Lynch JJ, Sitko GR, et al. Antithrombotic effects of MK-0852, a platelet fibrinogen receptor antagonist, in canine models of thrombosis. *J Pharmacol Exp Ther* 1993;266:1501–1511.

28. Scarborough RM, Naughton A, Teng W, et al. Design of potent and specific integrin antagonists. *J Biol Chem* 1993;268:1066–1073.

29. Cheng S, Craig WS, Mullen D, Tschopp JF, Dixon D, Pierschbacker MD. Design and synthesis of novel cyclic RGD-containing peptides as highly potent and selective integrin $\alpha_{IIb}\beta_3$ antagonists. *J Med Chem* 1994;37:1–9.

30. Mousa SA, Bozarth JM, Forsythe MS, et al. Antiplatelet and antithrombotic efficacy of DMP 728, a novel platelet GPIIb/IIIa receptor antagonist. *Circulation* 1994;89:3–12.

31. Dennis MS, Henzel WJ, Pitti RM, et al. Platelet glycoprotein IIb/IIIa protein antagonists from snake venoms: evidence for a family of platelet-aggregation inhibitors. *Proc Natl Acad Sci USA* 1989;87:2471–2475.

32. Charo IF, Kieffer N, Phillips DR. Platelet membrane glycoproteins. In: Coleman R, Hirsh J, Marder V, Salzman E, eds. *Hemostasis and thrombosis. Basic principles and clinical Practice*, 3rd ed. Philadelphia: JB Lippincott Co.; 1994:489–507.

33. Muto P, Lastoria S, Varrella P, Vergara E, Bernardy JD, Borer JS, Salvatore M. Detection of deep venous thrombosis by technetium-99m-labeled synthetic peptides P-280: preliminary results. *J Nucl Med* 1994;34:80P.

34. Muto P, Lastoria S, Varrella P, et al. Detection of deep venous thrombosis with technetium-99m-labeled synthetic peptide P280. *J Nucl Med* 1995;36:1384–1391.

NUCLEAR CARDIOLOGY

Influence of Downscatter in Simultaneously Acquired Thallium-201/Technetium-99m-PYP SPECT

Hiroshi Ando, Takaya Fukuyama, Wataru Mitsuoka, Shogo Egashira, Yoshihiro Imamura, Hiroyuki Masaki and Toshiaki Ashihara

Division of Cardiology, Matsuyama Red Cross Hospital, Matsuyama, Ehime, Japan

Simultaneously acquired dual-isotope imaging is a unique and useful approach in SPECT. Photon spillover, however, is a potential limitation of this technique. **Methods:** To investigate the degree of ^{99m}Tc downscatter into the ^{201}Tl window in patients, simultaneously acquired dual-isotope ^{201}Tl/^{99m}Tc-pyrophosphate imaging was performed in 17 patients with acute myocardial infarction (MI). Thallium-201 SPECT imaging was performed first, with a ^{201}Tl photopeak window after the ^{201}Tl injection (early ^{201}Tl images), followed by ^{99m}Tc injection and SPECT acquisition using dual-isotope windows (dual ^{201}Tl images). Twenty-four hours after the ^{99m}Tc injection, a third set of ^{201}Tl images was obtained (24-hr ^{201}Tl images). Thallium defect size (extent score) and defect severity (severity score) were calculated from these three sets of ^{201}Tl images to quantify the MI. **Results:** Technetium-99m accumulation of varying intensity was recognized in all patients. Extent scores and severity scores were identical in early ^{201}Tl images and 24-hr ^{201}Tl images. Both scores, however, in the dual ^{201}Tl images were decreased by 36% and 53%, respectively. **Conclusion:** There is a considerable ^{99m}Tc downscatter into the ^{201}Tl window, which prevents precise quantification of MI in simultaneously acquired dual-isotope ^{201}Tl/^{99m}Tc-pyrophosphate imaging.

Key Words: SPECT; simultaneous dual-isotope imaging; thallium-201; technetium-99m-pyrophosphate

J Nucl Med 1996; 37:781–785

The advent of new radiopharmaceuticals such as ^{99m}Tc myocardial perfusion imaging agents and ^{123}I-labeled compounds has provoked interest in simultaneously acquired dual-isotope imaging. This technique is advantageous because it can shorten the total acquisition time and reduce errors induced by image misalignment. In spite of these advantages, dual-isotope approaches could potentially cause images derived from the energy window of one radioisotope to be contaminated by spillover from the other tracer (downscatter). Analytical data regarding this downscatter in a clinical setting is limited (*1*). Yet simultaneous ^{201}Tl/^{99m}Tc-pyrophosphate dual-isotope SPECT has been commonly used in patients with acute myocardial infarction (MI) for diagnosing the location and size of infarctions without any downscatter correction.

Since ^{201}Tl-chloride concentrates in normally perfused myocardium and ^{99m}Tc-pyrophosphate concentrates in infarct zones, it might have been predicted that downscatter would not present a problem for this particular usage. The purpose of this study is to quantify the degree of the influence of ^{99m}Tc downscatter on ^{201}Tl images in simultaneously acquired ^{201}Tl/^{99m}Tc-pyrophosphate dual-isotope SPECT imaging in patients with acute myocardial infarction (MI).

MATERIALS AND METHODS

Patients

Thirty-two patients with acute MI who had been referred to our hospital between March 1991 and March 1992 were enrolled into this study. The patients with transmural MI were defined by the